

Cooling and state preparation in an optical lattice via Markovian feedback control

Ling-Na Wu* and André Eckardt†

Institut für Theoretische Physik, Technische Universität Berlin, Hardenbergstraße 36, Berlin 10623, Germany

(Dated: 5th October 2021)

We propose and investigate a scheme based on Markovian feedback control that allows for the preparation of single targeted eigenstates of a system of bosonic atoms in a one-dimensional optical lattice with high fidelity. It can be used for in-situ cooling the interacting system without particle loss, both for weak and strong interactions, and for experimentally preparing and probing individual excited eigenstates. For that purpose the system is assumed to be probed weakly via homodyne detection of photons that are scattered off-resonantly by the atoms from a structured probe beam into a cavity mode. By applying an inertial force to the system that is proportional to the measured signal, the system is then guided into a pure target state. The scheme is found to be robust against reduced measurement efficiencies.

Introduction.— Atomic quantum gases in optical lattices constitute a unique experimental platform for studying quantum many-body systems under extremely clean and flexible conditions [1]. An important property of these systems is their extremely high degree of isolation from the environment, which is provided by the optical trapping of atoms inside ultrahigh vacuum. It offers the rather unique opportunity to experimentally study coherent nonequilibrium dynamics of many-body systems [2] over hundreds of tunneling times, before eventually residual heating processes make themselves felt. However, suitable dissipation can also be beneficial and the lack of it a limitation. For instance, whenever excitations are created, e.g. by time-dependent parameter variations into a parameter regime of interest, the induced energy remains in the system and causes heating. Here the ability to cool the system after a parameter ramp *in situ* (without particle loss) would be highly desirable. Also the controlled preparation of states beyond the strict constraints of equilibrium in driven-dissipative systems offers intriguing perspectives, like the investigation of transport [3, 4], the engineering of non-hermitian Hamiltonians [5], Bose condensation in non-equilibrium steady states [6, 7], etc.. Therefore, various routes for engineering dissipation in quantum-gas experiments have been pursued already, such as the engineering of reservoirs [8] and heat baths [9], the implementation of dephasing noise via inelastic scattering of lattice photons [10], or engineered local particle loss/detection via ionization [11].

Here we propose and investigate a scheme for controlled dissipative state preparation and cooling in bosonic optical-lattice systems by means of measurement-based feedback control [12, 13]. It is based on the continuous measurement of photons that are off-resonantly scattered by the atoms from a structured probe beam into a cavity mode [14, 15] in combination with a simple lattice measurement-conditioned acceleration and can be used to prepare individual eigenstates of the system with high fidelity. Controlling the probe beam as well as the feedback strength allows for engineering an artificial environment with tailored properties. It permits preparing

the ground state (i.e. cooling) of the system with high fidelity not only for non or weakly interacting bosons, but, remarkably, at integer filling also for arbitrarily strong repulsion. Moreover, the approach is capable also of preparing individual excited eigenstates of the system, which would open the possibility to study their statistical properties as they are predicted, e.g., for ergodic systems by the eigenstate thermalization hypothesis (ETH) [16–18].

Measurement-based feedback control has been proposed and used already successfully in other systems for quantum state preparation [19–31], cooling [32–41], simulating nonlinear dynamics [42–44], as well as controlling dynamics [45–50] and phase transitions [51–55], just to name a few. In this paper, we consider Markovian feedback control as proposed by Wiseman [56], where a feedback Hamiltonian proportional to the measurement signal is continuously added to the system. It has been employed already for the stabilization of arbitrary one-qubit quantum states [57, 58], the control of two-qubit entanglement [59–62], as well as optical and spin squeezing [55, 63, 64].

Model.— We consider a system of N interacting bosonic atoms in a one-dimensional optical lattice described by the Bose-Hubbard model,

$$H = -J \sum_{l=1}^{M-1} (a_l^\dagger a_{l+1} + a_{l+1}^\dagger a_l) + \frac{U}{2} \sum_{l=1}^M n_l(n_l - 1), \quad (1)$$

with annihilation and number operators a_l and $n_l = a_l^\dagger a_l$ for bosons on site l . Here J quantifies nearest-neighbor tunneling and U on-site interactions.

In order to control the system via quantum feedback control, we consider a homodyne measurement of an operator c . The dynamical evolution of the system is then described by the stochastic master equation (SME) [12] ($\hbar = 1$ hereafter), $d\rho_c = -i[H, \rho_c]dt + \mathcal{D}[c]\rho_c dt + \mathcal{H}[c]\rho_c dW$, with $\mathcal{H}[c]\rho := c\rho + \rho c^\dagger - \text{Tr}[(c + c^\dagger)\rho]\rho$ and $\mathcal{D}[c]\rho := c\rho c^\dagger - \frac{1}{2}(c^\dagger c\rho + \rho c^\dagger c)$. Here ρ_c denotes the quantum state conditioned on the measurement result, $I_{\text{hom}} = \text{Tr}[(c+c^\dagger)\rho] + \xi(t)$, with $\xi(t) = dW/dt$ and dW being the standard Wiener increment with mean zero and

variance dt . The quantum backaction of a weak measurement can be used for tailoring the system's dynamics and state. For instance, a quantum nondemolition measurement of light allows for the preparation of different types of atom-number squeezed and macroscopic superposition states [15, 65]. Even more control is obtained by introducing measurement-dependent feedback.

Here we consider Markovian feedback control, where a feedback term $I_{\text{hom}}F$ proportional to the instantaneous signal is added to the Hamiltonian, giving rise to an evolution governed by the modified SME [56] $d\rho_c = -i[H + H_{\text{fb}}, \rho_c]dt + \mathcal{D}[A]\rho_c dt + \mathcal{H}[A]\rho_c dW$, with operators

$$A = c - iF, \quad H_{\text{fb}} = \frac{1}{2}(c^\dagger F + Fc). \quad (2)$$

Taking the ensemble average over the stochastic measurement outcomes gives the feedback-modified ME [56]

$$\dot{\rho} = -i[H + H_{\text{fb}}, \rho] + \mathcal{D}[A]\rho. \quad (3)$$

The effect induced by the feedback loop is seen to replace the collapse operator c by A and to add an extra term H_{fb} to the Hamiltonian. Our goal is to find the proper measurement operator c and feedback operator F so that the steady state of the ME (3) is (as close as possible to) an eigenstate $|E\rangle$ of the Hamiltonian H (1). Ref. [66] points out that the ME (3) has a pure steady state if and only if the effective Hamiltonian $H_{\text{eff}} = H + H_{\text{fb}} - iA^\dagger A/2$ and the collapse operator A have a common eigenstate, which is then the steady state. Since the additional feedback-induced term in the Hamiltonian H_{fb} is proportional to the measurement strength, for weak measurement, we can safely neglect H_{fb} relative to H and construct a collapse operator A so that $A|E\rangle = 0$. The dissipator cannot be neglected, since it is the only dissipative term. This strategy is confirmed in our simulations below, where H_{fb} is fully taken into account. In the following we will first discuss the preparation of the ground state $|G\rangle$, before considering also excited eigenstates.

Feedback scheme for non-interacting case.— In order to get an insight of how to choose the measurement and feedback operator, let us first take a look at the double-well system ($M = 2$). It can be mapped to a spin- $N/2$ system [67] with the collective spin operators defined as $J_x = \frac{1}{2}(a_1^\dagger a_2 + a_2^\dagger a_1)$, $J_y = -\frac{i}{2}(a_1^\dagger a_2 - a_2^\dagger a_1)$, and $J_z = \frac{1}{2}(a_1^\dagger a_1 - a_2^\dagger a_2)$, which are angular momentum operators satisfying the commutation relations $[J_\mu, J_\nu] = i\epsilon_{\mu\nu\sigma}J_\sigma$ for $\mu, \nu, \sigma = x, y, z$ and the Levi-Civita symbol $\epsilon_{\mu\nu\sigma}$. The ground state of the non-interacting Hamiltonian $H_2 = -J(a_1^\dagger a_2 + a_2^\dagger a_1) = -2JJ_x$ is the eigenstate of J_x , $|j = N/2, m = N/2\rangle$, with the largest eigenvalue $m = N/2$. From the theory of angular momentum, we know that this state is also an eigenstate of operator $J_- = J_z - iJ_y$ with eigenvalue 0. Hence, by choosing the measurement operator c as $\sqrt{\gamma}J_z$ and feedback operator F as $\sqrt{\gamma}J_y$, so that $A = \sqrt{\gamma}(J_z - iJ_y)$, we will reach a steady state

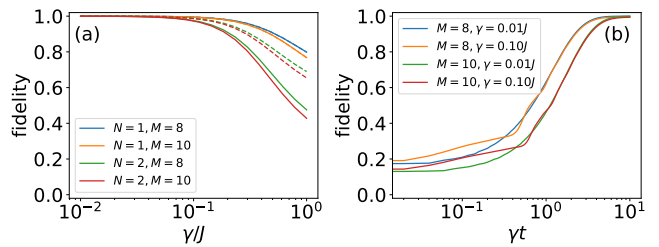


Figure 1. (a) Fidelities f (solid) and \tilde{f} (dashed) between the steady state of Eq. (3) and the ground state of Eq. (1) versus measurement strength γ . (b) Fidelity between the instantaneous state and the ground state of Eq. (1), starting from the state with one particle on the leftmost site.

very close to the ground state of the Hamiltonian H_2 for weak measurement with strength $\gamma \ll J$.

Generalizing this scenario to the multi-site case, we consider the measurement and feedback operator

$$c = \sqrt{\gamma} \sum_{l=1}^M z_l n_l, \quad F = \sqrt{\gamma} \sum_{l=1}^{M-1} (i a_{l+1}^\dagger a_l - i a_l^\dagger a_{l+1}). \quad (4)$$

Here c is a weighted sum of site occupations and can be implemented via homodyne detection of the off-resonant scattering of structured probe light from the atoms [14, 15, 68]. The detection efficiency can be enhanced by placing the system inside an optical cavity [14, 50, 69–71], so that via the Purcell effect [72] the photons are scattered predominantly into one cavity mode. The feedback F is given by an imaginary component of the tunneling parameter and can be realized by accelerating the lattice, as discussed below. For the non-interacting case ($U = 0$), the ground state of (1) reads $|G\rangle = \frac{1}{\sqrt{N!}} (\sum_l g_l a_l^\dagger)^N |0\rangle$ with $g_l = \sqrt{\frac{2}{M+1}} \sin(\frac{\pi l}{M+1})$. The condition $A|G\rangle = (c - iF)|G\rangle = 0$ then fixes the coefficients in the measurement operator to $z_l = (g_{l+1} - g_{l-1})/g_l$.

In order to check the proposed scheme, we calculate the fidelity f between the steady state ρ_{ss} of Eq. (3) and the ground state $|G\rangle$ of Eq. (1), i.e., $f = \sqrt{\langle G | \rho_{\text{ss}} | G \rangle}$, which takes values between 0 and 1. To compare results for different particle numbers, we also introduce the fidelity “per particle” $\tilde{f} \equiv f^{1/N}$. Figure 1(a) shows the fidelity as a function of the measurement strength γ . As expected, for small enough γ , H_{fb} has no detrimental impact and a close-to-one fidelity is approached [73]. This is confirmed when considering the excitation energy $\Delta E = \text{Tr}[\rho_{\text{ss}} H] - \langle G | H | G \rangle$ as a probe of deviations from the target state [74]. In the presence of an external trapping potential, the scheme can directly be adapted, simply by replacing the coefficients g_l by the discrete single-particle ground-state wavefunction of trapped system and even without being adapted it is robust against weak potential modulations (see [74] for more details).

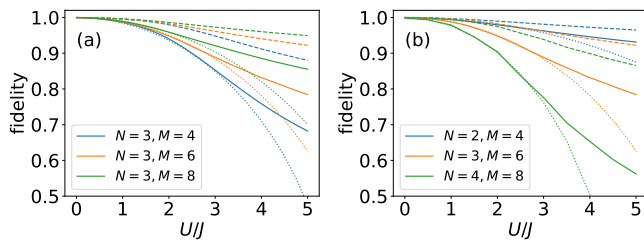


Figure 2. Steady state fidelities f (solid) and \tilde{f} (dashed) versus interaction strength U for different site numbers M at (a) $N = 3$ and (b) half filling $N = M/2$, with $\gamma = 0.01J$. The dotted lines denote the fitting curves $f^2 = 1 - \chi[(nU)/(2\Delta E)]^2$ with χ being the fitting parameter [74].

The coupling γ also influences the time required to reach the steady state. For one particle in a double-well system ($N = 1$, $M = 2$), it is easy to verify that $f^2 = 1 - \frac{1}{2}e^{-4\gamma t}$ [74]. Hence, a close-to-one fidelity can be reached at $\gamma t \gtrsim 1$. In Fig. 1(b), we show the time-dependent fidelity $f = \sqrt{\langle G|\rho(t)|G \rangle}$ as a function of the scaled time γt for $N = 1$. For $\gamma t \gtrsim 1$ the curves for different γ collapse and quickly approach the steady state. From Fig. 1 we can infer that $\gamma \lesssim 0.1J$ is sufficient to achieve a high fidelity, corresponding to a preparation in a few tens of tunnelling times. For a larger system (with larger M or N) smaller γ and thus also longer times are required [74].

Without any modification the feedback scheme still performs well in the presence of weak interactions $U \lesssim J$, as can be seen from Fig. 2 showing the steady-state fidelity versus U . While for fixed total particle number N the scheme works better for larger system sizes (M) [Fig. 2(a) for $N = 3$], the opposite trend is observed when instead fixing the filling $n = N/M$ [see Fig. 2(b) for $n = 1/2$].

Feedback scheme for interacting particles.— To better capture the impact of interactions, we adapt the feedback scheme by adding a prefactor λ to the feedback operator F , so that the collapse operator becomes

$$A = c - i\lambda F, \quad (5)$$

The choice of λ maximizing the fidelity is shown in Fig. 3(a) as a function of U . The corresponding fidelity is shown in (b). We can observe that in the case of integer filling (orange line), this simple rescaling of the feedback strength allows to achieve fidelities close to unity for all interaction strengths. The fact that it is possible to prepare the ground state of an interacting system for every interaction strength, including the strongly correlated regime of intermediate interactions close to the Mott transition [75], is remarkable, especially since we are considering only single-particle (i.e. quadratic) measurement and feedback operators c and F and since it is sufficient to vary a single parameter λ to cover the whole range of interactions.

This choice (5) can again be motivated by inspecting the double-well case. For weak interactions, the

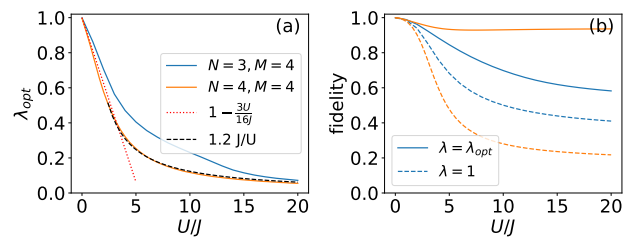


Figure 3. (a) The optimal parameter λ which gives the highest fidelity between the steady state of Eq. (3) and the ground state of Eq. (1) as a function of the interaction strength U . The corresponding fidelity f is shown in (b) for $\gamma = 0.01J$.

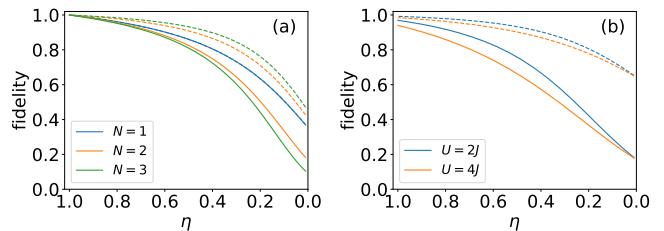


Figure 4. Steady-state fidelities f (solid) and \tilde{f} (dashed) as a function of the detection efficiency η for (a) non-interacting case with different particle number N at $M = 8$ and for (b) interacting case with $M = N = 4$ and $\gamma = 0.01J$.

ground state is given by $|G\rangle \simeq |\psi_0^{(0)}\rangle - \alpha|\psi_2^{(0)}\rangle$ where $|\psi_n^{(0)}\rangle$ denotes the n th eigenstate of the non-interacting Hamiltonian and $\alpha = \sqrt{2N(N-1)}(U/J)/16$. Since $A|G\rangle \propto [\sqrt{N}(1-\lambda) - \alpha\sqrt{2(N-1)}(1+\lambda)]|\psi_1^{(0)}\rangle$, the cooling condition can be satisfied by setting $\lambda = 1 - (U/J)(N-1)/(4M)$, which is a linear function of U/J . For integer filling, the ansatz (5) is also suitable for strong interactions. The ground state is then approximated by $|G\rangle \simeq |n, n\rangle + (nJ/U)(|n+1, n-1\rangle + |n-1, n+1\rangle)$ with integer $n = N/2$. This gives $A|G\rangle = \sqrt{\gamma}[n_1 - n_2 - \lambda(a_1^\dagger a_2 - a_2^\dagger a_1)]|G\rangle \simeq \sqrt{\gamma}n(2J/U - \lambda)(|n+1, n-1\rangle - |n-1, n+1\rangle)$. Therefore, by setting $\lambda = 2J/U$, we have $A|G\rangle \simeq 0$, which leads to a steady state close to the ground state of the system. For half-integer filling (odd N), the condition $A|G\rangle \simeq 0$ does not hold for any λ [74]. Generalizing this reasoning to M sites, we again find $\lambda \propto U/J$ for weak interactions and for integer filling also $\lambda \propto J/U$ for strong interactions [dashed and dotted lines in Fig. 3(a)].

Imperfect detection efficiency.— So far, we have assumed perfect detection, $\eta = 1$. For an efficiency $\eta < 1$, the ME becomes [56] $\dot{\rho} = -i[H + H_{\text{fb}}, \rho] + \mathcal{D}[A]\rho + \frac{1-\eta}{\eta}\mathcal{D}[F]\rho$. In Fig. 4, we investigate the robustness against a reduction of η . For both the non-interacting (a) and the interacting (b) cases, the fidelity is found to decrease slowly with η . Roughly speaking, large fidelities require efficiencies larger than 50 percent.

Stabilizing excited eigenstates.— It is also possible to prepare excited eigenstates of the system. For the

single-particle problem, the n th eigenstate reads $|\psi_n\rangle = \sum_l g_l^{(n)} |l\rangle$, with $g_l^{(n)} = \sqrt{\frac{2}{M+1}} \sin\left(\frac{n\pi l}{M+1}\right)$, with $n = 1, 2, \dots, M$. We can stabilize each of these eigenstates as steady state by using the feedback and measurement operators (4) with $z_l = [g_{l+1}^{(n)} - g_{l-1}^{(n)}]/g_l^{(n)}$. This scheme can be generalized to N non-interacting particles to prepare the n th “coherent” eigenstate $|n, N\rangle = \frac{1}{\sqrt{N!}} (\sum_l g_l^{(n)} a_l^\dagger)^N |0\rangle$, where all particles occupy the n th single-particle eigenstate. Figure 5(a) shows the fidelities between the steady state and $|n, N\rangle$ versus γ . By symmetry states $|n, N\rangle$ and $|M - n + 1, N\rangle$ show the same behavior. As expected, the fidelity increases and approaches 1 as γ decreases. The preparation of states closer to the center of the spectrum requires smaller γ .

The preparation of excited eigenstates of the interacting system offers the intriguing perspective to study their individual properties experimentally. This would allow, for instance, to directly probe ETH [16–18], stating that each individual eigenstate of a generic ergodic system is characterized by expectation values that follow the prediction of the microcanonical ensemble. In Fig. 5(b) we plot the mean occupations $\langle n_0 \rangle$ of the leftmost site for all eigenstates of a system with $N = 4$, $M = 15$, and $U = J$ and one can see that the data points mostly form a rather thin stripe, confirming that (up to finite size effects) the expectation values depend mainly on the energy. Since it turns out that the stabilization of excited eigenstates via feedback control is difficult for the interacting system, we propose to use feedback control for the preparation of non-interacting eigenstates $|n, N\rangle$ and to then linearly switch on the interactions via a Feshbach resonance in a second step. In Fig. 5(c), we plot the overlap of the time evolved states for a ramp time of $T = 100/J$ with the interacting many-body eigenstates $|k\rangle$. The energy expected for perfect adiabatic behaviour is indicated by the vertical dashed lines of the same color in Fig. 5(b). While for initial coherent eigenstates with smaller energy, we find a very narrow distribution with almost only a single eigenstate occupied, for larger energies broader distributions indicate non-adiabatic behaviour. We attribute the latter to the dynamic instability caused by the combination of repulsive interactions with negative effective mass found for states with large kinetic energy [76]. Even broader distributions are found [74], when preparing the state via a quench from a state with every other site occupied like in a recent experiment [77]. After the interaction ramp, we let the prepared state evolve with the interacting Hamiltonian and plot the mean-occupation versus time [Fig. 5(d), colors like in (c)]. The fact that we hardly see any evolution of that expectation value for the states with the lower energies, shows how close they are to an eigenstate. In turn, for the prepared states in the upper half in the spectrum we find strong oscillations indicating the superposition of a few eigenstates.

Experimental implementation.— By including the

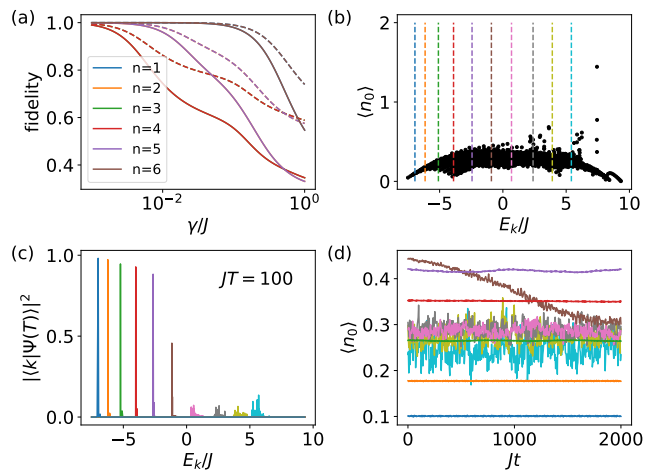


Figure 5. (a) Fidelities f (solid) and \tilde{f} (dashed) between the steady state of Eq. (3) and the n th “coherent” eigenstate $|n, N\rangle$ versus γ for $N = 2$, $M = 6$, $U = 0$. (b) The expectation value of n_0 in the eigenstates at $U = J$. The dashed lines mark the states corresponding to $|n, N\rangle$. (c) The distribution of the final state from adiabatic preparation (with the interaction strength U linearly ramped up from 0 to J within $JT = 100$ starting from the corresponding “coherent” eigenstate at $U = 0$) on the eigenbasis at $U = J$. (d) Evolution of $\langle n_0 \rangle$ under the Hamiltonian (1) with $U = J$ starting from the final state from adiabatic preparation. $N = 4$ and $M = 15$ in (b)-(d).

feedback control term $I_{\text{hom}}F$ to the Hamiltonian (1), the parameter for tunneling (rightwards) is modified to $J' = J + i\sqrt{\gamma}I_{\text{hom}} = \sqrt{J^2 + \gamma I_{\text{hom}}^2} e^{i\theta(t)}$, with $\tan \theta(t) = \sqrt{\gamma}I_{\text{hom}}/J$. This can be achieved by accelerating the lattice potential $V_L(x)$ according to $V(x, t) = V_L(x - d_L \xi(t))$, with d_L being the lattice constant. In the reference frame co-moving with the lattice, the corresponding inertial force is described by a time-dependent vector potential represented by the time-dependent Peierls phase $\theta(t) = md_L^2 \dot{\xi}(t)$ attached to the tunneling matrix element [78]. Now choose $\dot{\xi}(t) = \arctan(\sqrt{\gamma}I_{\text{hom}}/J)/(md_L^2) = \frac{2E_R}{\pi^2} \arctan(\sqrt{\gamma}I_{\text{hom}}/J)$ with $E_R = \pi^2/(2md_L^2)$.

The drift of lattice $\xi(t)$ is dependent on the homodyne current I_{hom} , and can be simulated from solving the modified SME. We show the standard deviation of the lattice displacement (in unit of d_L), $\Delta\xi(t)$, in Fig. 6(a) (blue solid line), with $E_R/J = 15$ corresponding to a lattice depth of $V_0/E_R \approx 5$ [79]. $\Delta\xi(t)$ is found to be proportional to $\sqrt{\gamma t}$, a feature of a random walk. At the time when the system approaches the steady state [Fig. 6(b)], the average drift of the lattice is about $1.5d_L$. The drift can be reduced further without losing fidelity by postselecting those trajectories with $\xi(t)$ remaining below a given threshold (dashed and dotted lines).

Conclusion.—We have proposed and investigated a simple scheme for measurement-based feedback control of a system of ultracold bosonic atoms in an optical lattice. Remarkably, at integer filling a simple modification

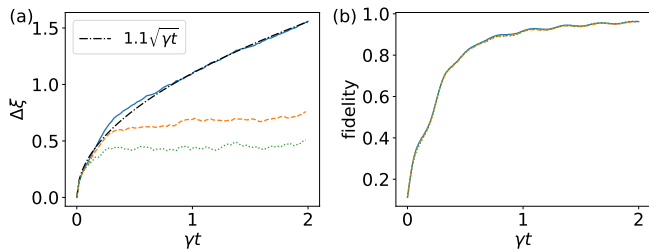


Figure 6. (a) Standard deviation $\Delta\xi$ of lattice drift ξ versus time, averaged either over all 1000 trajectories of the SME (solid) or over a postselected ensemble [dashed(dotted)], where the 50%(85%) of the trajectories were discarded that reach $\xi > 1.8$ (1.2) during the evolution. (b) Corresponding fidelities between the instantaneous state and the ground state. The parameters are $N = 2$, $M = 4$, $U = J$, $dt = 0.01/J$, $\gamma = 0.1J$. Initially all atoms occupy the leftmost site.

of the feedback strength allows for cooling the system at arbitrary repulsive interaction strengths. Moreover, we showed that it is possible to prepare individual excited eigenstates, which would allow to experimentally study their statistical properties as they are predicted by the ETH. As an outlook, it will be interesting to generalize the scheme predicted here to scenarios, where *in situ* cooling would be crucial, in order to counteract heating caused by Floquet engineering or imperfect adiabatic state preparation at a quantum phase transition, e.g. for the preparation of topological quantum states. Moreover, also the engineering of artificial thermal baths via feedback control, mimicking finite-temperature reservoirs and the combination of two of them to study heat-current-carrying steady states in a highly controllable quantum gas is a fascinating perspective. Generally, it will be interesting to employ feedback control to realize driven-dissipative systems and to control the properties of their non-equilibrium steady states (or phases) beyond the constraints of thermal equilibrium.

We acknowledge discussions with Lorenz Wanckel and Tobias Donner. This research was funded by the Deutsche Forschungsgemeinschaft (DFG, German Research Foundation) Projektnummer 163436311 SFB 910.

* lingna.wu@tu-berlin.de

† eckardt@tu-berlin.de

- [1] Maciej Lewenstein, Anna Sanpera, and Veronica Ahufinger, *Ultracold Atoms in Optical Lattices: Simulating quantum many-body systems* (Oxford University Press, 2012).
- [2] Anatoli Polkovnikov, Krishnendu Sengupta, Alessandro Silva, and Mukund Vengalattore, “Colloquium: Nonequilibrium dynamics of closed interacting quantum systems,” *Rev. Mod. Phys.* **83**, 863–883 (2011).
- [3] Gabriel T. Landi, Dario Poletti, and Gernot Schaller, “Non-equilibrium boundary driven quantum

- systems: models, methods and properties,” (2021), arXiv:2104.14350 [quant-ph].
- [4] B. Bertini, F. Heidrich-Meisner, C. Karrasch, T. Prosen, R. Steinigeweg, and M. Žnidarič, “Finite-temperature transport in one-dimensional quantum lattice models,” *Rev. Mod. Phys.* **93**, 025003 (2021).
 - [5] Emil J. Bergholtz, Jan Carl Budich, and Flore K. Kunst, “Exceptional topology of non-hermitian systems,” *Rev. Mod. Phys.* **93**, 015005 (2021).
 - [6] Daniel Vorberg, Waltraut Wustmann, Roland Ketzmerick, and André Eckardt, “Generalized bose-einstein condensation into multiple states in driven-dissipative systems,” *Phys. Rev. Lett.* **111**, 240405 (2013).
 - [7] Alexander Schnell, Daniel Vorberg, Roland Ketzmerick, and André Eckardt, “High-temperature nonequilibrium bose condensation induced by a hot needle,” *Phys. Rev. Lett.* **119**, 140602 (2017).
 - [8] Sebastian Krinner, Tilman Esslinger, and Jean-Philippe Brantut, “Two-terminal transport measurements with cold atoms,” *Journal of Physics: Condensed Matter* **29**, 343003 (2017).
 - [9] Felix Schmidt, Daniel Mayer, Quentin Bouton, Daniel Adam, Tobias Lausch, Nicolas Spethmann, and Artur Widera, “Quantum spin dynamics of individual neutral impurities coupled to a bose-einstein condensate,” *Phys. Rev. Lett.* **121**, 130403 (2018).
 - [10] H. Pichler, A. J. Daley, and P. Zoller, “Nonequilibrium dynamics of bosonic atoms in optical lattices: Decoherence of many-body states due to spontaneous emission,” *Phys. Rev. A* **82**, 063605 (2010).
 - [11] Herwig Ott, “Single atom detection in ultracold quantum gases: a review of current progress,” *Reports on Progress in Physics* **79**, 054401 (2016).
 - [12] Howard M Wiseman and Gerard J Milburn, *Quantum measurement and control* (Cambridge university press, 2009).
 - [13] Jing Zhang, Yu-xi Liu, Re-Bing Wu, Kurt Jacobs, and Franco Nori, “Quantum feedback: theory, experiments, and applications,” *Physics Reports* **679**, 1–60 (2017).
 - [14] Helmut Ritsch, Peter Domokos, Ferdinand Brennecke, and Tilman Esslinger, “Cold atoms in cavity-generated dynamical optical potentials,” *Rev. Mod. Phys.* **85**, 553–601 (2013).
 - [15] T. J. Elliott, W. Kozłowski, S. F. Caballero-Benitez, and I. B. Mekhov, “Multipartite entangled spatial modes of ultracold atoms generated and controlled by quantum measurement,” *Phys. Rev. Lett.* **114**, 113604 (2015).
 - [16] Marcos Rigol, Vanja Dunjko, and Maxim Olshanii, “Thermalization and its mechanism for generic isolated quantum systems,” *Nature* **452**, 854–858 (2008).
 - [17] Adam M Kaufman, M Eric Tai, Alexander Lukin, Matthew Rispoli, Robert Schittko, Philipp M Preiss, and Markus Greiner, “Quantum thermalization through entanglement in an isolated many-body system,” *Science* **353**, 794–800 (2016).
 - [18] Luca D’Alessio, Yariv Kafri, Anatoli Polkovnikov, and Marcos Rigol, “From quantum chaos and eigenstate thermalization to statistical mechanics and thermodynamics,” *Advances in Physics* **65**, 239–362 (2016).
 - [19] Antonio Negretti, Uffe V. Poulsen, and Klaus Mølmer, “Quantum superposition state production by continuous observations and feedback,” *Phys. Rev. Lett.* **99**, 223601 (2007).
 - [20] Andrew C. J. Wade, Jacob F. Sherson, and Klaus

- Mølmer, “Squeezing and entanglement of density oscillations in a bose-einstein condensate,” *Phys. Rev. Lett.* **115**, 060401 (2015).
- [21] Jonas Lammers, Hendrik Weimer, and Klemens Hammerer, “Open-system many-body dynamics through interferometric measurements and feedback,” *Phys. Rev. A* **94**, 052120 (2016).
- [22] JM Geremia, “Deterministic and nondestructively verifiable preparation of photon number states,” *Phys. Rev. Lett.* **97**, 073601 (2006).
- [23] Masahiro Yanagisawa, “Quantum feedback control for deterministic entangled photon generation,” *Phys. Rev. Lett.* **97**, 190201 (2006).
- [24] Clément Sayrin, Igor Dotsenko, Xingxing Zhou, Bruno Peaudecerf, Théo Rybarczyk, Sébastien Gleyzes, Pierre Rouchon, Mazhar Mirrahimi, Hadis Amini, Michel Brune, Jean-Michel Raimond, and Serge Haroche, “Real-time quantum feedback prepares and stabilizes photon number states,” *Nature* **477**, 73–77 (2011).
- [25] X. Zhou, I. Dotsenko, B. Peaudecerf, T. Rybarczyk, C. Sayrin, S. Gleyzes, J. M. Raimond, M. Brune, and S. Haroche, “Field locked to a fock state by quantum feedback with single photon corrections,” *Phys. Rev. Lett.* **108**, 243602 (2012).
- [26] JM Geremia, John K. Stockton, and Hideo Mabuchi, “Real-time quantum feedback control of atomic spin-squeezing,” *Science* **304**, 270–273 (2004).
- [27] Ryotaro Inoue, Shin-Ichi-Ro Tanaka, Ryo Namiki, Takahiro Sagawa, and Yoshiro Takahashi, “Unconditional quantum-noise suppression via measurement-based quantum feedback,” *Phys. Rev. Lett.* **110**, 163602 (2013).
- [28] Kevin C. Cox, Graham P. Greve, Joshua M. Weiner, and James K. Thompson, “Deterministic squeezed states with collective measurements and feedback,” *Phys. Rev. Lett.* **116**, 093602 (2016).
- [29] M. Gajdacz, A. J. Hilliard, M. A. Kristensen, P. L. Pedersen, C. Klempt, J. J. Arlt, and J. F. Sherson, “Preparation of ultracold atom clouds at the shot noise level,” *Phys. Rev. Lett.* **117**, 073604 (2016).
- [30] D. Ristè, M. Dukalski, C. A. Watson, G. de Lange, M. J. Tiggeleman, Ya. M. Blanter, K. W. Lehnert, R. N. Schouten, and L. DiCarlo, “Deterministic entanglement of superconducting qubits by parity measurement and feedback,” *Nature* **502**, 350–354 (2013).
- [31] V. Sudhir, D. J. Wilson, R. Schilling, H. Schütz, S. A. Fedorov, A. H. Ghadimi, A. Nunnenkamp, and T. J. Kippenberg, “Appearance and disappearance of quantum correlations in measurement-based feedback control of a mechanical oscillator,” *Phys. Rev. X* **7**, 011001 (2017).
- [32] M. Schemmer, A. Johnson, R. Photopoulos, and I. Bouchoule, “Monte carlo wave-function description of losses in a one-dimensional bose gas and cooling to the ground state by quantum feedback,” *Phys. Rev. A* **95**, 043641 (2017).
- [33] M R Hush, S S Szigeti, A R R Carvalho, and J J Hope, “Controlling spontaneous-emission noise in measurement-based feedback cooling of a bose-einstein condensate,” *New Journal of Physics* **15**, 113060 (2013).
- [34] S. S. Szigeti, M. R. Hush, A. R. R. Carvalho, and J. J. Hope, “Continuous measurement feedback control of a bose-einstein condensate using phase-contrast imaging,” *Phys. Rev. A* **80**, 013614 (2009).
- [35] Vladan Vuletić, James K. Thompson, Adam T. Black, and Jonathan Simon, “External-feedback laser cooling of molecular gases,” *Phys. Rev. A* **75**, 051405 (2007).
- [36] L. S. Walker, G. R. M. Robb, and A. J. Daley, “Measurement and feedback for cooling heavy levitated particles in low-frequency traps,” *Phys. Rev. A* **100**, 063819 (2019).
- [37] D A Ivanov and T Yu Ivanova, “Bragg-reflection-based feedback cooling of optically trapped particles,” *Journal of Physics B: Atomic, Molecular and Optical Physics* **47**, 135303 (2014).
- [38] Pavel Bushev, Daniel Rotter, Alex Wilson, François Dubin, Christoph Becher, Jürgen Eschner, Rainer Blatt, Viktor Steixner, Peter Rabl, and Peter Zoller, “Feedback cooling of a single trapped ion,” *Phys. Rev. Lett.* **96**, 043003 (2006).
- [39] Markus Koch, Christian Sames, Alexander Kubanek, Matthias Apel, Maximilian Balbach, Alexei Ourjoumtsev, Pepijn W. H. Pinkse, and Gerhard Rempe, “Feedback cooling of a single neutral atom,” *Phys. Rev. Lett.* **105**, 173003 (2010).
- [40] N. Behbood, G. Colangelo, F. Martin Ciurana, M. Napolitano, R. J. Sewell, and M. W. Mitchell, “Feedback cooling of an atomic spin ensemble,” *Phys. Rev. Lett.* **111**, 103601 (2013).
- [41] D. J. Wilson, V. Sudhir, N. Piro, R. Schilling, A. Ghadimi, and T. J. Kippenberg, “Measurement-based control of a mechanical oscillator at its thermal decoherence rate,” *Nature* **524**, 325–329 (2015).
- [42] Seth Lloyd and Jean-Jacques E. Slotine, “Quantum feedback with weak measurements,” *Phys. Rev. A* **62**, 012307 (2000).
- [43] Manuel H. Muñoz Arias, Pablo M. Poggi, Poul S. Jessen, and Ivan H. Deutsch, “Simulating nonlinear dynamics of collective spins via quantum measurement and feedback,” *Phys. Rev. Lett.* **124**, 110503 (2020).
- [44] Manuel H. Muñoz Arias, Ivan H. Deutsch, Poul S. Jessen, and Pablo M. Poggi, “Simulation of the complex dynamics of mean-field p -spin models using measurement-based quantum feedback control,” *Phys. Rev. A* **102**, 022610 (2020).
- [45] Alexander Carmele, Julia Kabuss, Franz Schulze, Stephan Reitzenstein, and Andreas Knorr, “Single photon delayed feedback: A way to stabilize intrinsic quantum cavity electrodynamics,” *Phys. Rev. Lett.* **110**, 013601 (2013).
- [46] R. Vijay, C. Macklin, D. H. Slichter, S. J. Weber, K. W. Murch, R. Naik, A. N. Korotkov, and I. Siddiqi, “Stabilizing rabi oscillations in a superconducting qubit using quantum feedback,” *Nature* **490**, 77–80 (2012).
- [47] N. V. Morrow, S. K. Dutta, and G. Raithel, “Feedback control of atomic motion in an optical lattice,” *Phys. Rev. Lett.* **88**, 093003 (2002).
- [48] Daniel A. Steck, Kurt Jacobs, Hideo Mabuchi, Tanmoy Bhattacharya, and Salman Habib, “Quantum feedback control of atomic motion in an optical cavity,” *Phys. Rev. Lett.* **92**, 223004 (2004).
- [49] T. Vanderbruggen, R. Kohlhaas, A. Bertoldi, S. Bernon, A. Aspect, A. Landragin, and P. Bouyer, “Feedback control of trapped coherent atomic ensembles,” *Phys. Rev. Lett.* **110**, 210503 (2013).
- [50] Katrin Kroeger, Nishant Dogra, Rodrigo Rosa-Medina, Marcin Paluch, Francesco Ferri, Tobias Donner, and Tilman Esslinger, “Continuous feedback on a quantum gas coupled to an optical cavity,” *New Journal of Physics* **22**, 033020 (2020).

- [51] Wassilij Kopylov, Clive Emary, Eckehard Schöll, and Tobias Brandes, “Time-delayed feedback control of the dicke–hepp–lieb superradiant quantum phase transition,” *New Journal of Physics* **17**, 013040 (2015).
- [52] D. A. Ivanov, T. Yu. Ivanova, S. F. Caballero-Benitez, and I. B. Mekhov, “Feedback-induced quantum phase transitions using weak measurements,” *Phys. Rev. Lett.* **124**, 010603 (2020).
- [53] Hilary M. Hurst, Shangjie Guo, and I. B. Spielman, “Feedback induced magnetic phases in binary bose-einstein condensates,” *Phys. Rev. Research* **2**, 043325 (2020).
- [54] Hilary M. Hurst and I. B. Spielman, “Measurement-induced dynamics and stabilization of spinor-condensate domain walls,” *Phys. Rev. A* **99**, 053612 (2019).
- [55] Giuseppe Buonaiuto, Federico Carollo, Beatriz Olmos, and Igor Lesanovsky, “Dynamical phases and quantum correlations in an emitter-waveguide system with feedback,” arXiv e-prints , arXiv:2102.02719 (2021), arXiv:2102.02719 [quant-ph].
- [56] H. M. Wiseman, “Quantum theory of continuous feedback,” *Phys. Rev. A* **49**, 2133–2150 (1994).
- [57] Jin Wang and H. M. Wiseman, “Feedback-stabilization of an arbitrary pure state of a two-level atom,” *Phys. Rev. A* **64**, 063810 (2001).
- [58] P. Campagne-Ibarcq, S. Jezouin, N. Cottet, P. Six, L. Bretheau, F. Mallet, A. Sarlette, P. Rouchon, and B. Huard, “Using spontaneous emission of a qubit as a resource for feedback control,” *Phys. Rev. Lett.* **117**, 060502 (2016).
- [59] Jin Wang, H. M. Wiseman, and G. J. Milburn, “Dynamical creation of entanglement by homodyne-mediated feedback,” *Phys. Rev. A* **71**, 042309 (2005).
- [60] A. R. R. Carvalho and J. J. Hope, “Stabilizing entanglement by quantum-jump-based feedback,” *Phys. Rev. A* **76**, 010301 (2007).
- [61] A. R. R. Carvalho, A. J. S. Reid, and J. J. Hope, “Controlling entanglement by direct quantum feedback,” *Phys. Rev. A* **78**, 012334 (2008).
- [62] L. C. Wang, J. Shen, and X. X. Yi, “Effect of feedback control on the entanglement evolution,” *The European Physical Journal D* **56**, 435–440 (2010).
- [63] P. Tombesi and D. Vitali, “Physical realization of an environment with squeezed quantum fluctuations via quantum-nondemolition-mediated feedback,” *Phys. Rev. A* **50**, 4253–4257 (1994).
- [64] L. K. Thomsen, S. Mancini, and H. M. Wiseman, “Spin squeezing via quantum feedback,” *Phys. Rev. A* **65**, 061801 (2002).
- [65] Igor B. Mekhov and Helmut Ritsch, “Quantum nondemolition measurements and state preparation in quantum gases by light detection,” *Phys. Rev. Lett.* **102**, 020403 (2009).
- [66] Naoki Yamamoto, “Parametrization of the feedback hamiltonian realizing a pure steady state,” *Phys. Rev. A* **72**, 024104 (2005).
- [67] BJ Dalton and S Ghanbari, “Two mode theory of bose-einstein condensates: interferometry and the josephson model,” *Journal of Modern Optics* **59**, 287–353 (2012).
- [68] Yuto Ashida and Masahito Ueda, “Diffraction-unlimited position measurement of ultracold atoms in an optical lattice,” *Phys. Rev. Lett.* **115**, 095301 (2015).
- [69] Ferdinand Brennecke, Tobias Donner, Stephan Ritter, Thomas Bourdel, Michael Köhl, and Tilman Esslinger, “Cavity qed with a bose–einstein condensate,” *Nature* **450**, 268–271 (2007).
- [70] Renate Landig, Ferdinand Brennecke, Rafael Mottl, Tobias Donner, and Tilman Esslinger, “Measuring the dynamic structure factor of a quantum gas undergoing a structural phase transition,” *Nature communications* **6**, 1–6 (2015).
- [71] Farokh Mivehvar, Francesco Piazza, Tobias Donner, and Helmut Ritsch, “Cavity QED with Quantum Gases: New Paradigms in Many-Body Physics,” arXiv e-prints , arXiv:2102.04473 (2021), arXiv:2102.04473 [cond-mat.quant-gas].
- [72] Edward Mills Purcell, “Spontaneous emission probabilities at radio frequencies,” in *Confined Electrons and Photons* (Springer, 1995) pp. 839–839.
- [73] For odd site number M , the steady state is not unique due to degeneracies in the spectrum. However, by adding tiny interactions a unique steady state is recovered.
- [74] See Supplementary Material, which includes Ref. [80], for the calculation of the fidelity for one particle in a double well, discussion of the nonunique steady state for odd site number, energy difference between the steady state and the ground state, feedback scheme in the presence of an external potential, the robustness of the free particle scheme against disorder, the system size dependence of the measurement strength, perturbation theory for the double well system under weak interactions, discussion about double well system with odd particle numbers and multi-site case (general M) at integer filling, and state distribution in the eigenbasis.
- [75] Subir Sachdev and Markus Müller, “Quantum criticality and black holes,” *Journal of Physics: Condensed Matter* **21**, 164216 (2009).
- [76] Oliver Morsch and Markus Oberthaler, “Dynamics of bose-einstein condensates in optical lattices,” *Rev. Mod. Phys.* **78**, 179–215 (2006).
- [77] S. Trotzky, Y.-A. Chen, A. Flesch, I. P. McCulloch, U. Schollwöck, J. Eisert, and I. Bloch, “Probing the relaxation towards equilibrium in an isolated strongly correlated one-dimensional bose gas,” *Nature Physics* **8**, 325–330 (2012).
- [78] André Eckardt, “Colloquium: Atomic quantum gases in periodically driven optical lattices,” *Rev. Mod. Phys.* **89**, 011004 (2017).
- [79] Immanuel Bloch, Jean Dalibard, and Wilhelm Zwerger, “Many-body physics with ultracold gases,” *Rev. Mod. Phys.* **80**, 885–964 (2008).
- [80] Serge Aubry and Gilles André, “Analyticity breaking and anderson localization in incommensurate lattices,” *Proceedings, VIII International Colloquium on Group-Theoretical Methods in Physics* **3** (1980).

Supplementary Material

Ling-Na Wu and André Eckardt

Institut für Theoretische Physik, Technische Universität Berlin, Hardenbergstraße 36, Berlin 10623, Germany

ONE PARTICLE IN A DOUBLE WELL

For one particle in a double well, the system Hamiltonian reads

$$H = \begin{pmatrix} 0 & -J \\ -J & 0 \end{pmatrix}, \quad (\text{S1})$$

whose ground state is given by $|G\rangle = \frac{1}{\sqrt{2}} \begin{pmatrix} 1 \\ 1 \end{pmatrix}$. The feedback master equation (ME) reads

$$\dot{\rho} = -i[H, \rho] + \mathcal{D}[A]\rho, \quad (\text{S2})$$

with the collapse operator given by

$$A = \sqrt{\gamma}(\sigma_z - i\sigma_y) = \sqrt{\gamma} \begin{pmatrix} 1 & -1 \\ 1 & -1 \end{pmatrix}. \quad (\text{S3})$$

Note that the additional feedback-induced term in the Hamiltonian $H_{\text{fb}} \propto \{\sigma_y, \sigma_z\} = 0$ in this case.

Starting from the initial state $\begin{pmatrix} 1 \\ 0 \end{pmatrix}$, the state at time t is given by

$$\rho(t) = \frac{1}{2} \begin{pmatrix} 1 + e^{-2\gamma t} \cos(2Jt) & 1 - e^{-4\gamma t} - ie^{-2\gamma t} \sin(2Jt) \\ 1 - e^{-4\gamma t} + ie^{-2\gamma t} \sin(2Jt) & 1 - e^{-2\gamma t} \cos(2Jt) \end{pmatrix}. \quad (\text{S4})$$

Hence, we have

$$\langle G|\rho(t)|G\rangle = 1 - \frac{1}{2}e^{-4\gamma t}. \quad (\text{S5})$$

THE NONUNIQUE STEADY STATE FOR ODD SITE NUMBER (M) CASE

For the non-interacting case, when the site number M is odd, the steady state of the system is not unique. This is attributed to the presence of more than one dark state of the collapse operator A due to the degeneracy of the system. To better understand it, we can take a look at an example with $M = 3$ and $N = 2$. There are three single-particle eigenstates in this case, with energies $E_{-1} = -\sqrt{2}J$, $E_0 = 0$, $E_1 = \sqrt{2}J$. Therefore, the system has two degenerate eigenstates with eigenenergy 0, i.e., one state with two particles in state $|E_0\rangle$, and one state with one particle in $|E_1\rangle$ and the other in $|E_{-1}\rangle$. When expressed in the Fock state representation of the eigenstate basis, $|n_{-1}, n_0, n_{-1}\rangle$, these two states read $|0, 2, 0\rangle$ and $|1, 0, 1\rangle$. Any superposition of these two states is also an eigenstate of the system, $|\psi\rangle = \alpha|0, 2, 0\rangle + \beta|1, 0, 1\rangle$. Both components will be pumped to the state $|1, 1, 0\rangle$ by the collapse operator A . A proper choice of the coefficients α and β will then lead to $A|\psi\rangle = 0$. Namely, besides the ground state $|2, 0, 0\rangle$, there is another dark state of A . Therefore, if the initial state has an overlap with this dark state, this component will not be influenced by the action of A and remain the same during the evolution. In this case, the steady state won't be the ground state of the system. The key point in the above reasoning is the degeneracy of the system, which leads to the appearance of other dark states (besides the ground state) due to the 'destructive' interference between the degenerate eigenstates. When such a degeneracy is lifted, for instance, by including interactions, the steady state becomes unique (the ground state). When the site number is even, it can be shown that the ground state is the only dark state of A in spite of the degeneracy of the system.

ENERGY DIFFERENCE BETWEEN THE STEADY STATE AND THE GROUND STATE

As a second measure of the effectiveness of our cooling scheme, we calculate the energy difference between the steady state and the ground state ΔE , normalized by the width of the spectrum ($E_{\text{max}} - E_{\text{min}}$). The results are shown in Fig. S1.

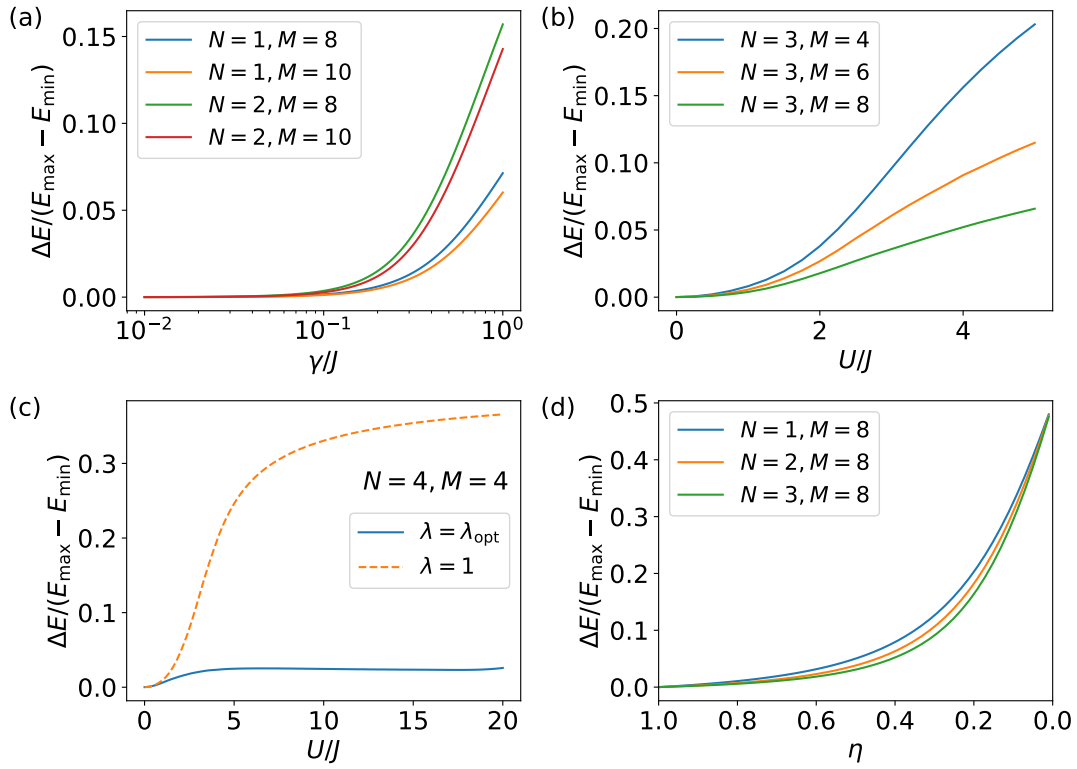


Figure S1. The energy difference between the steady state and the ground state ΔE normalized by the width of the spectrum ($E_{\max} - E_{\min}$), as a function of (a) the measurement strength γ with $U = 0$, (b)-(c) the interaction strength U , and (d) the detection efficiency η with $U = 0$. The measurement strength in (b)-(d) is $\gamma = 0.01J$. In (a), (b), and (d), $\lambda = 1$. (c) compares the results with $\lambda = 1$ and the optimized λ_{opt} .

EXTERNAL TRAPPING POTENTIAL

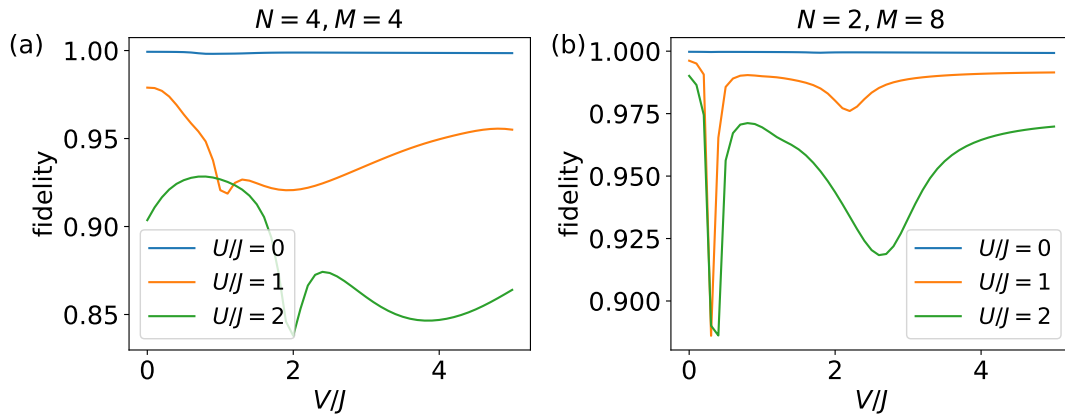


Figure S2. The fidelity between the steady state and the ground state as a function of the potential strength V .

Here we consider the case when there is an external harmonic trapping potential

$$H_V = \frac{V}{2} \sum_{l=1}^M (l - l_0)^2 n_l, \quad (\text{S6})$$

with $l_0 = (M - 1)/2$. To cool the system in this case, one should use measurement operator $c = \sum_l z_l n_l$ with $z_l = [g_{l+1} - g_{l-1}]/g_l$ and g_l being the coefficient of the ground state for the system with the on-site potential. Figure S2 shows the fidelity between the steady state and the ground state as a function of the potential strength V . We can see that for the non-interacting systems, a close-to-one fidelity can be obtained no matter how strong the potential is. For the interacting systems, the fidelity is degraded due to the potential, but the influence is found to be weak.

THE ROBUSTNESS OF THE FREE PARTICLE SCHEME AGAINST DISORDER

As a test of the robustness of the free particle scheme, we add quasi disorder via an incommensurate periodic potential modulation (Aubry-André model [80]) $V(l) = V_d \cos(2\pi\beta l)$, with $\beta = (\sqrt{5} - 1)/2$, i.e., consider the Hamiltonian

$$H = -J \sum_l (a_l^\dagger a_{l+1} + a_{l+1}^\dagger a_l) + \sum_l V(l) n_l, \quad (\text{S7})$$

and see how the fidelity decreases with the disorder strength V_d . The results are shown in Fig. S3, where V_d remains below the critical value of $V_d^c = 2J$, so that all eigenstates remain delocalized. We can see that the scheme is robust to weak disorder.

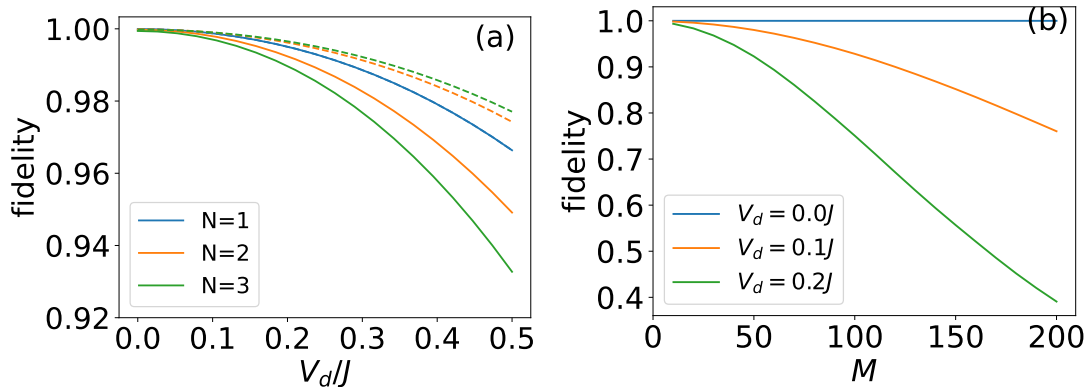


Figure S3. The fidelities f (solid) and \tilde{f} (dashed) between the steady state of the proposed scheme and the ground state of Eq. (S7) as a function of (a) the disorder strength V_d for different N at $M = 8$, and (b) the system size M at $N = 1$. Other parameters are $U = 0$, $\gamma = 0.01J$.

SYSTEM SIZE DEPENDENCE OF THE MEASUREMENT STRENGTH γ

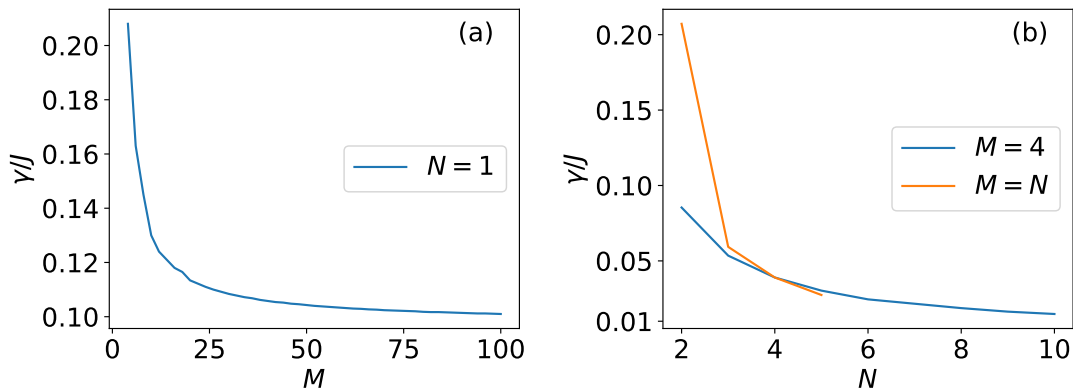


Figure S4. The maximal measurement strength γ needed to reach a fidelity of 0.99 as a function of (a) M with $N = 1$, and (b) N with $M = 4$ or $M = N$. The interaction strength is $U = 0$.

Here we consider the system size dependence of the measurement strength γ . The fidelity increases as the measurement strength γ decreases. Figure S4 shows the maximal γ to reach a fidelity of 0.99 for various system sizes. From (a), one can see that the dependence of γ on M is weak when N is fixed. As for the dependence on N [see (b)], γ shows a fast decay with increasing N at the beginning and then the decrease becomes slow as N increases further.

DOUBLE WELL SYSTEM UNDER WEAK INTERACTIONS

According to perturbation theory, for weak interactions $NU/2 \ll J$, the ground state is approximately given by $|G\rangle \simeq |\psi_0^{(0)}\rangle - \alpha|\psi_2^{(0)}\rangle$, where $|\psi_n^{(0)}\rangle$ denotes the n th eigenstate of the non-interacting Hamiltonian and $\alpha = \sqrt{2N(N-1)}(U/J)/16$. By noting $J_-|\psi_2^{(0)}\rangle = \sqrt{2(N-1)}|\psi_1^{(0)}\rangle$ and $J_-|\psi_1^{(0)}\rangle = \sqrt{N}|\psi_0^{(0)}\rangle$, we see that the ground state is coupled to the first excited state $|E\rangle \simeq |\psi_1^{(0)}\rangle$ by the collapse operator $A = \sqrt{\gamma}J_-$ and the ratio of transfer rate between them reads $|\langle E|J_-|G\rangle/\langle G|J_-|E\rangle|^2 = [\sqrt{2(N-1)}\alpha/\sqrt{N}]^2 = [(N-1)(U/J)/8]^2 \equiv \nu$, the fidelity is approximately given by $f^2 = 1 - \nu$. For general M , the scenario is more complicated as the ground state is coupled to several states, while the conclusion is generally that the reduction of the fidelity is proportional to $[nU/(2\Delta E)]^2$ with the filling factor $n = N/M$ and single-particle energy gap $\Delta E = 2J \cos[\pi/(M+1)] - 2J \cos[2\pi/(M+1)]$.

DOUBLE WELL SYSTEM WITH ODD PARTICLE NUMBERS

For odd N and $M = 2$, when $U \gg NJ$, the ground state is approximately given by

$$|G\rangle \simeq \frac{1}{\sqrt{2}} \left(\left| \frac{N+1}{2}, \frac{N-1}{2} \right\rangle + \left| \frac{N-1}{2}, \frac{N+1}{2} \right\rangle \right) + \frac{NJ}{4\sqrt{2}U} \left(\left| \frac{N+3}{2}, \frac{N-3}{2} \right\rangle + \left| \frac{N-3}{2}, \frac{N+3}{2} \right\rangle \right). \quad (\text{S8})$$

Therefore, for $N \gg 1$ we have

$$\begin{aligned} \frac{1}{\sqrt{\gamma}}A|G\rangle &= [n_1 - n_2 - \lambda(a_1^\dagger a_2 - a_2^\dagger a_1)]|G\rangle \\ &\simeq \frac{1}{\sqrt{2}} \left(\left| \frac{N+1}{2}, \frac{N-1}{2} \right\rangle - \left| \frac{N-1}{2}, \frac{N+1}{2} \right\rangle \right) + \frac{3NJ}{4\sqrt{2}U} \left(\left| \frac{N+3}{2}, \frac{N-3}{2} \right\rangle - \left| \frac{N-3}{2}, \frac{N+3}{2} \right\rangle \right) \\ &\quad - \frac{\lambda N}{2\sqrt{2}} \left(\left| \frac{N+3}{2}, \frac{N-3}{2} \right\rangle + \left| \frac{N+1}{2}, \frac{N-1}{2} \right\rangle \right) - \frac{\lambda N^2 J}{8\sqrt{2}U} \left(\left| \frac{N+5}{2}, \frac{N-5}{2} \right\rangle + \left| \frac{N-1}{2}, \frac{N+1}{2} \right\rangle \right) \\ &\quad + \frac{\lambda N}{2\sqrt{2}} \left(\left| \frac{N-1}{2}, \frac{N+1}{2} \right\rangle + \left| \frac{N-3}{2}, \frac{N+3}{2} \right\rangle \right) + \frac{\lambda N^2 J}{8\sqrt{2}U} \left(\left| \frac{N+1}{2}, \frac{N-1}{2} \right\rangle + \left| \frac{N-5}{2}, \frac{N+5}{2} \right\rangle \right) \\ &= |G\rangle + \frac{\lambda N}{2\sqrt{2}} \left(\frac{NJ}{4U} - 1 \right) \left(\left| \frac{N+1}{2}, \frac{N-1}{2} \right\rangle - \left| \frac{N-1}{2}, \frac{N+1}{2} \right\rangle \right) \\ &\quad + \frac{N}{2\sqrt{2}} \left(\frac{J}{U} - \lambda \right) \left(\left| \frac{N+3}{2}, \frac{N-3}{2} \right\rangle - \left| \frac{N-3}{2}, \frac{N+3}{2} \right\rangle \right) \\ &\quad - \frac{\lambda N^2 J}{8\sqrt{2}U} \left(\left| \frac{N+5}{2}, \frac{N-5}{2} \right\rangle - \left| \frac{N-5}{2}, \frac{N+5}{2} \right\rangle \right). \end{aligned} \quad (\text{S9})$$

From above expression, we can see that it's impossible to make $A|G\rangle = 0$ no matter what value λ takes. We can only make the transfer rate from the ground state to other states small by setting $\lambda = J/U$.

MULTI-SITE CASE (GENERAL M) AT INTEGER FILLING

Now let's consider the general M case with integer filling factor $n = N/M$. For $U \gg NJ$, the ground state is well approximated by

$$|G\rangle \simeq |n, \dots, n\rangle + \frac{nJ}{U} \sum_{l=1}^{M-1} (|n, \dots, n_l + 1, n_{l+1} - 1, \dots, n\rangle + |n, \dots, n_l - 1, n_{l+1} + 1, \dots, n\rangle), \quad (\text{S10})$$

where the second term contains all the Fock states that can be obtained from the equally distributed state $|n, \dots, n\rangle$ by transferring one particle from one site to its neighboring site. This gives

$$\frac{1}{\sqrt{\gamma}}c|G\rangle = \sum_{l=1}^M z_l n_l |G\rangle \simeq \frac{nJ}{U} \sum_{l=1}^{M-1} (z_l - z_{l+1}) (|n, \dots, n_l + 1, n_{l+1} - 1, \dots, n\rangle - |n, \dots, n_l - 1, n_{l+1} + 1, \dots, n\rangle), \quad (\text{S11})$$

where we have used $\sum_l z_l = 0$, and

$$\frac{i}{\sqrt{\gamma}}F|G\rangle = \sum_{l=1}^{M-1} (a_l^\dagger a_{l+1} - a_{l+1}^\dagger a_l)|G\rangle \simeq n \sum_{l=1}^{M-1} (|n, \dots, n_l + 1, n_{l+1} - 1, \dots, n\rangle - |n, \dots, n_l - 1, n_{l+1} + 1, \dots, n\rangle). \quad (\text{S12})$$

Therefore,

$$\frac{1}{\sqrt{\gamma}}A|G\rangle = \frac{1}{\sqrt{\gamma}}(c - i\lambda F)|G\rangle \simeq n \sum_{l=1}^{M-1} \left[(z_l - z_{l+1}) \frac{J}{U} - \lambda \right] (|n, \dots, n_l + 1, n_{l+1} - 1, \dots, n\rangle - |n, \dots, n_l - 1, n_{l+1} + 1, \dots, n\rangle). \quad (\text{S13})$$

So by setting $\lambda = (z_l - z_{l+1}) \frac{J}{U}$, we have $A|G\rangle \simeq 0$.

STATE DISTRIBUTION IN THE EIGENBASIS

Figure S5 shows the distribution of some states, which can be prepared experimentally, in the eigenbasis at $U = J$. (a) shows the ground states at various interaction strength U . One can see that all of them have a large overlap with the low energy states. (b) shows the state with every second site occupied. This state has a broad distribution with a center in the middle of the spectrum.

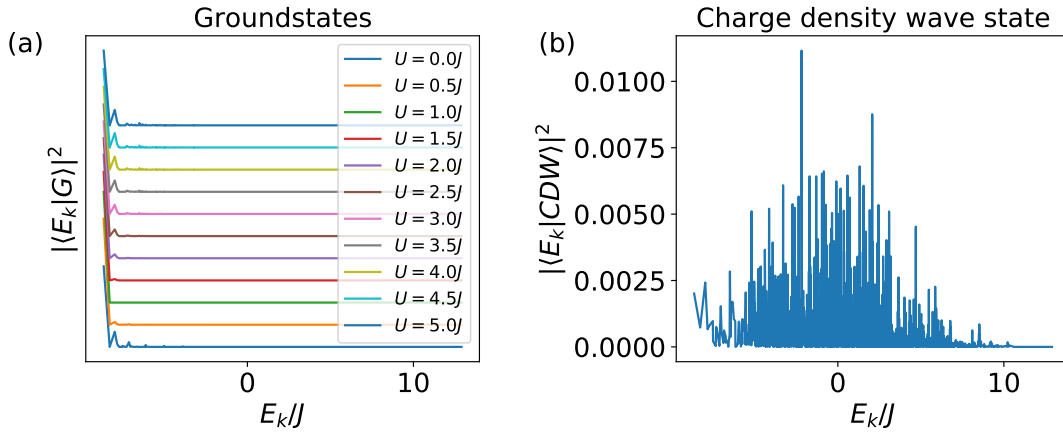


Figure S5. The distribution of some states in the eigenbasis at $U = J$. (a) The ground states at various interaction strength U . (b) The charge density wave state with every second site occupied. The system sizes are $N = 5$ and $M = 10$.